Magnetohydrodynamic Nonlinear Radiative Heat and Mass Transfer Flow of Sisko nanofluid through a Nonlinear Stretching Sheet in The Presence of Chemical Reaction

Abstract: The problem of heat and mass transfer of Sisko nanofluid flowing through a nonlinear stretching sheet under the influence of chemical reaction, heat source, magnetohydrodynamics, and thermal radiation is examined in this study. The controlling model equations are rendered dimensionless, and the resulting set of nonlinear ordinary differential equations are solved utilizing the shooting technique for the nondimensional velocity, temperature, and concentration profiles, along with Runge-Kutta-Fehlberg's method of fourth order. Using symbolic software MAPLE, the properties of numerous relevant parameters, including the chemical reaction parameter, Lewis number, thermophoresis parameter, Brownian motion parameter, Biot number, material parameter of the Sisko fluid, magnetic field parameter, power law index, radiation parameter and generalized Prandtl numberare presented graphically and quantifiably discussed. Further, the local Sherwood number and the local Nusselt numbers are calculated, presented in the table, and compared with existing literature. The results of our investigation show that the Sisko fluid's material properties increase the velocity profile, while increase in magnetic field and chemical reaction decrease it. In the same vein, the temperature distribution of the fluid decreases with increasing magnetic field, Biot number, thermophoresis parameter, and Lewis number, but increases when chemical reaction occurs. Concentration profiles are augmented by positive increases in the magnetic field and Brownian motion, but they plunge with increases in Lewis numbers, Biot numbers, chemical reactions, and thermophoresis parameters.

Keywords. Magnetohydrodynamics**,** Nonlinear Sheet, Chemical reaction, Sisko nanofliud, Heat and mass transfer

1. Introduction

Sisko nanofluid is a specific kind of nanofluid that displays shear-thinning behavior, whose viscosity decreases as the shear rate rises. Excellent heat transmission capabilities of Sisko nanofluid have been demonstrated, making it appropriate for use in cooling systems, heat exchangers, and electronic devices, among other applications. [1]. The unique characteristic of Sisko nanofluid lies in its rheological behavior. Traditional nanofluids, such as those derived from water or oil, frequently display Newtonian behavior, where the viscosity remains constant with shear rate. Sisko nanofluid, on the other hand, differs from this pattern of behavior and demonstrates shear-thinning characteristics. This indicates that when the shear rate rises, the viscosity of the substance falls, improving the flow and heat transfer properties [2]. The existence of surface-modified nanoparticles and their interactions with the base fluid are attributed for the Sisko nanofluid's shear-thinning characteristic. Reduced viscosity is the result of the fluid's network-like structure, which the nanoparticles create, disintegrating under shear stress. As a result, the efficiency of heat transmission is increased [3]. This behavior makes it easier to pump through and

flow via small channels. The temperature and flow properties of the Sisko nanofluid have been studied in many investigations. According to research studies, Sisko nanofluids, compared to conventional fluids, can greatly increase the heat transmission coefficient. They have also been discovered to have better thermal conductivity, which improves the efficiency of their heat transfer. [4]. Khan and Shahzad [5] obtained analytical solution to only integral values of the power-law index for the boundary layer equations of a Sisko fluid through a flat stretched surface. Malik et al. [6] investigated the partial slip effects on the flow and heat transfer of an incompressible Sisko fluid over a nonlinear stretching sheet and stretching cylinder with variable thermal conductivity.

Several industrial and technical operations in the fields of metallurgy and chemical engineering are affected by heat transport phenomena in a laminar boundary layer flow across a stretching sheet. Numerous researchers have examined the flow past a stretching surface with various stretching velocities, including linear, exponential, quadratic, hyperbolic, radially, and even oscillatory. [7, 8, 9]. However, there are only a few studies on the transfer of heat and mass in laminar boundary layer flow through a nonlinear stretching sheet. It is widely known in literature that stretching in many industrial applications is not always linear, for this reason academics have studied nonlinear stretching sheets for various fluid flows. Rashidi et al. [10] conducted a lie group analysis to examined freeconvective flow of a nanofluid through a horizontal porous plate in the presence of chemical reaction. The mixed convective heat and mass transport of nanofluids over a nonlinear stretching sheet under the influence of suction/injection parameter, magnetic parameter, and thermophoresis parameter has been studied by Mondal et al. [11] in their analysis. The shooting technique has used by Dhanai et al. [12] to investigate the impact of viscous dissipation for the problem of magneto-hydrodynamic boundary layer flow of nanofluid that results from a power-law stretching/shrinking permeable sheet. The problem of boundary layer flow of nanofluid through nonlinear permeable stretching sheet at specified surface temperature in the presence of partial slip has been investigated numerically by Das [13]. Megahed et al. [14] have researched on the significance of thermal buoyancy and continuous heat flux on the steady two-dimensional flow and heat transfer of non-Newtonian power-law fluid under the influence of thermal radiation.The two-dimensional boundary layer flow of a viscous, incompressible, and electrically conducting fluid over a nonlinearly stretching non-isothermal sheet in the presence of a variable transverse magnetic field, thermal radiation, viscous dissipation, and a nonlinearly moving free stream was studied numerically by Kumbhakar and Rao [15]. The motion of MHD heat and mass transfer of nanofluid due to a stretching sheet through a porous medium with radiation effect was implemented by Reddy et al. [16]Many technical processes, such as nuclear power plants, gas turbines, and the numerous propulsion systems for airplanes, missiles, satellites, and spacecraft, use heat transfer, which is

influenced by thermal radiation. It is important to note that the nonlinear approximation problem is controlled by three parameters, including the Prandtl number, radiation parameter, and temperature ratio parameter, whereas the linearized Rosseland approximation only uses the effective Prandtl number as a dimensionless parameter. Krishnamurthy et al. [17] considered the magnetohydrodynamic and nonlinear radiative heat transfer of Sisko nanofluid through a nonlinear stretching sheet under the influence of chemical reaction. The problem of Sisko liquid over a stretching surface in the presence of nonlinear thermal radiation, chemical reaction and magnetic field has been perused by Nagendramma [18]. A flat plate with partial slip at the surface subjected to the convective heat flux in the presence of nonlinear thermal radiation was explored by Parida et al. [19] for two-dimensional steady MHD boundary layer flow of heat and mass transfer. The boundary layer flow induced by a continuous stretched sheet in a quiet fluid in the presence of nonlinear Rosseland thermal radiation was the subject of a computational approach carried out by Cortell [20]. Using a novel radiation parameter known as the film radiation parameter, Pantokratoras [21] examined the impact of linear and nonlinear Rosseland radiation on steady laminar natural convection down a vertical isothermal plate.

Equally, non-Newtonian nanofluids have gained prominence during the past year because of their industrial applications. It has been demonstrated previously that the use of a working fluid containing nanoparticles may significantly improve the efficiency and performance of heat transfer phenomena. Numerous studies have placed emphasis on non-Newtonian fluid over a stretched sheet as the basic fluid with dispersed nanoparticles. For instance, the effects of thermophoresis and Brownian motion on the flow of Jeffrey nanofluid in a three-dimensional boundary layer and convective heat transfer through a bidirectional stretching surface were investigated by Hayat et al. [22] utilizing a recently developed boundary condition with zero nanoparticle mass flux. In the presence of thermal radiation, Brownian motion, and thermophoresis effects, Khan et al. [23]have implemented the impact of convective boundary conditions on two-dimensional boundary layer flow and heat transfer of Sisko nanofluid over a nonlinearly stretching sheet.Mabood et al. [24] have researched the consequences ofnon-uniform heat sources on steady two-dimensional hydromagnetic mixed convective heat and mass transfer flow of a micropolar fluid over a stretching sheet embedded in a non-Darcian porous medium with thermal radiation, variable thermal conductivity, Soret parameter andviscous-Ohmic dissipation.Heat and mass transfer of two-phase nanofluid flow in a rotating system in the presence of a transverse magnetic field have been addressed analytically by Ebiwareme et al. [25] using an Adomian decomposition approach. It was found in their study, that the pertinent parameters have profound influence on the flow distributions. Masood et al. [26] studied the flow of heat transfer on Sisko nanofluid across a nonlinear stretching

sheet. The influence of thermal radiation on the convective heat and mass transfer flow of a Sisko nanofluid across a nonlinear stretching sheet has been taken into consideration by Venkata et al. [27]. Mansood Khan et al. [28] has investigated the flow and heat transfer of Sisko fluid incorporating convective boundary condition through a non-isothermal stretching sheet using Homotopy analysis method in comparison with the exact solution. Using Homotopy analysis method along with the shooting technique, analysis of forced convective heat transfer in a boundary layer flow of Sisko fluid over a nonlinear stretching sheet with variable temperature and heat flux boundary conditions has been addressed by Asif Munir et al. [29].Pal and Mandal [30] has numerically studied the stagnation-point flow of a Sisko nanofluid through a stretching sheet on the impression of suction, magnetohydrodynamics, joules heating and viscous dissipation. The characteristics of radiation, magnetic field, and thermo-diffusion on nano fluid over a stretching sheet has been analytically researched by Mahmood et al. [31]. A numerical study of heat and mass transfer flow viscous nanofluid via a convective stretching sheet with the influence of chemical reaction, magnetohydrodynamics, viscous dissipation and thermal radiation has been perused by Narender et al. [32]. MHD boundary flow and heat transfer to Sisko nanofluid through a nonlinear stretching sheet under the impression of radiation has been considered by Gireesha et al. [33]. Ankita and Singh [34] have examined a mathematical model and heat transfer of magnetohydrodynamics Sisko nanofluid due to solar radiation through a stretching sheet in the presence of heat source and thermal conductivity using the nanofluid as a working fluid in the Solar collector. The effect of Newtonian heating on the flow of power-law nanofluid over a stretching surface has been theoretically addressed by Hayat et al. [35]

In this present study, ourmain objective is to add the novelty of concentration based internal heat source on the heat and mass transfer flow of Sisko nanofluid through a nonlinear stretching sheet under the impression ofchemical reaction, magnetohydrodynamics and nonlinear Rosseland approximation. Using fourth order Runge-Kutta-Felberg method along with the shooting technique, the solution for velocity, temperature and concentration profiles and their graphical representations are obtained using MAPLE boundary value subroutine as they are influenced by thermophoresis parameter, Brownian motion parameter, Biot number, magnetic field parameter, radiation parameter, chemical reaction parameter, Lewis number, generalized Prandtl number, material parameter of the Sisko fluid, and power law index.The study is categorized as follows. In section one, introduction of the study exploring exhaustive literatures for possible gaps in the study is given. The mathematical formulation comprising the governing equation as well as the reduction of the governing boundary layer equations subject to the prescribed boundary conditions using self-similar transformation is presented in section two. In the next section, solution to the

nondimensionalised equation for the flow distributions including Nusselt and Sherwood numbers are implemented using MAPLE Solver. Section four gives the presentation of the results for different values of the pertinent parameters presented in graphs and figures. The conclusion of the study highlighting the major outcomes is given in section five.

2. Mathematical Formulations

We examine a laminar, two-dimensional, continuous flow of a Sisko nanofluid in the domain $y > 0$, induced by a stretching sheet with a power-law velocity profile,$U = cx^s$. Here, c denotes a non-negative real constant and $s > 0$ represents the rate at which the sheet is stretched. The temperature of the stretched surface and nanoparticles are considered to be constant variables, represented by T_w andC_w, respectively. When y tends to infinity, the ambient values of temperature and nanoparticle fraction are denoted by T_∞ and C_∞, respectively. The magnetic field is applied normally to the stretching sheet. The flow is along the x-axis, while the y-axis is normal to the plane of the sheet, as shown in figure 1 below. Essentially, the fixed temperature and nanoparticle fraction for the stretching surface are presumed greater than the ambient temperature and nanoparticle fraction.

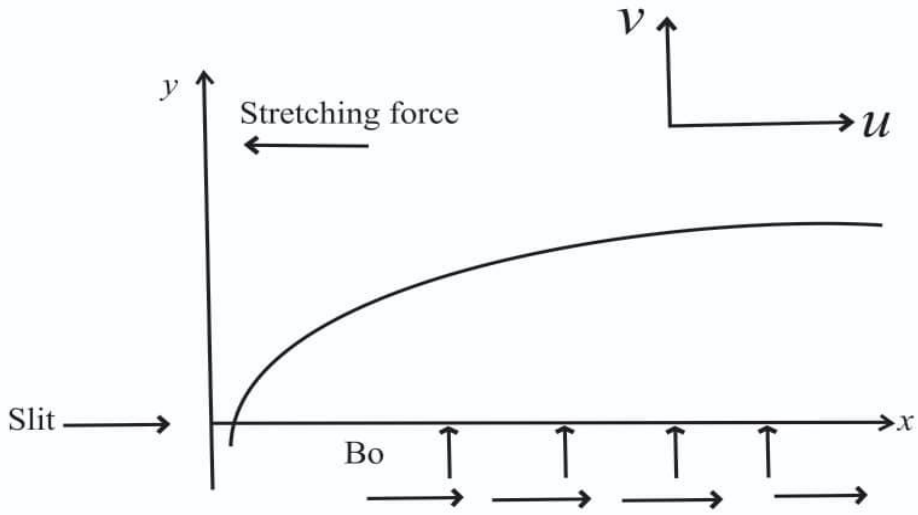

Figure 1.Physical configuration of the model

In the context of the assumptions stated herein, the appropriate governing equationsfollowing [27]

$$\frac{\partial u}{\partial x} + \frac{\partial v}{\partial y} = 0 \qquad (1)$$

$$u\frac{\partial u}{\partial x} + v\frac{\partial u}{\partial y} = \frac{\alpha}{\rho}\frac{\partial^2 u}{\partial y^2} - \frac{b}{\rho}\frac{\partial}{\partial y}\left(-\frac{\partial u}{\partial y}\right)^r - \frac{\sigma B_0^2}{\rho}u \qquad (2)$$

$$u\frac{\partial T}{\partial x} + v\frac{\partial T}{\partial y} = \frac{\partial}{\partial y}\left(\alpha + \frac{16\sigma^* T_\infty^3}{3\rho C_P k^*}\right)\frac{\partial T}{\partial y} + \tau\left[D_B\frac{\partial C}{\partial y}\frac{\partial T}{\partial y} + \frac{D_T}{T_\infty}\left(\frac{\partial T}{\partial y}\right)^2\right] \qquad (3)$$

$$u\frac{\partial C}{\partial x}+v\frac{\partial C}{\partial y}=D_B\frac{\partial^2 C}{\partial y^2}+\frac{D_T}{T_\infty}\frac{\partial^2 T}{\partial y^2}-k_1(C_w-C_\infty) \quad (4)$$

The associated boundary conditions prescribed in this problem are given as

$$u(x,y)=U=cx^s, v(x,y)=0, k\frac{\partial T(x,y)}{\partial y}=-h_f\left(T_f-T(x,y)\right) \text{at } y=0$$

$$D_B\frac{\partial C(x,y)}{\partial y}=-k_m\left(C_f-C(x,y)\right) \quad (5)$$

$u\longrightarrow 0, T\longrightarrow T_w, C\longrightarrow C_\infty$ as $y\longrightarrow\infty$

Let u and v denote the velocity components along the x and y axes, respectively. The material constants of the Sisko fluid are represented by a, b, and r ($r\geq 0$), T refers to the temperature of the fluid, C is the mass concentration of the solid nanoparticle volume fraction, $\rho, \sigma, \alpha, and k$ are the fluid density, electrical conductivity, thermal diffusivity, and thermal conductivity, $D_B$denotes the Brownian motion diffusion coefficient and$D_T$represent the thermophoresis coefficient.

The non dimensionless velocity, temperature and the nanoparticles fraction volume are defined as follows.

$$f'=\frac{u}{U}, \theta=\frac{T-T_\infty}{T_f-T_\infty}, \varphi=\frac{C-C_\infty}{C_f-C_\infty} \quad (6)$$

where$T-T_\infty$, $T_f-T_\infty, C-C_\infty$, C_f-C_∞ are the fluid temperature, and the concentration of Sisko nanoparticles respectively.Following [27], we define the similarity transformationgroup given by

$$\eta=\frac{y}{x}Re_b^{\frac{1}{r+1}}, v(x,y)=-URe_b^{\frac{1}{r+1}}\frac{1}{r+1}[\{s(2r-1)+1\}f(\eta)+\{s(2-r)-1\}\eta f'(\eta)],$$

$$u(x,y)=Uf'(\eta) \quad (7)$$

The non dimensional variables are given as

$$Re_a=\frac{\rho xU}{a}, Re_b=\frac{\rho x^r U^{2-r}}{b}, \text{A}=\frac{Re_b^{\frac{2}{r+1}}}{Re_a}, P=\frac{XU}{\alpha}Re_b^{\frac{2}{r+1}}, \ B_{i_1}=\frac{h_f}{k}xRe_bB=\frac{\tau D_B(C_f-C_\infty)}{\alpha}, \ T_p=$$

$$\frac{\tau D_T(T_f-T_\infty)}{T_\infty\alpha}, \ Le=\frac{\alpha}{D_B}, B_{i_2}=\frac{h_m}{k}xRe_b^{\frac{-1}{r+1}}, \ \text{R}=\frac{16\sigma\text{T}_\infty^3}{3\text{k}\rho\text{C}_\text{p}}, k_1=\frac{\gamma a}{Le}D_B=\frac{\propto}{Le}M=\frac{Re_a\sigma B_0^2}{Re_b^{\frac{1}{r+1}}}, \gamma=\frac{k_1Le}{a} \quad (8)$$

Using Eqs(6), (7) and (8), the governing Eqs. (1−4) reduced to the form.

$$Af'''+r(-f'')^{r-1}f'''+\left(\frac{s(2r-1)+1}{r+1}\right)ff''-sf'^2-Mf' \quad (9)$$

$$\left(\frac{1}{1+R}\right)\theta''+P\left(\frac{s(2r-1)+1}{r+1}\right)f\theta'+B\varphi'\theta'+T_p\theta'^2=0 \quad (10)$$

$$\varphi'' + Le\left(\frac{s(2r-1)+1}{r+1}\right) f\varphi' + \frac{T_p}{B}\theta'' - \gamma\varphi = 0 \qquad (11)$$

The corresponding transformed boundary conditions are given asfollows.

$$f(0) = 0, f'(0) = 1, \theta'(0) = -B_{i_1}[1 - \theta(0)], \varphi(0) = 1$$

$$f' \to 0, \theta \to 0, \varphi \to 0 \; as \; \eta \to \infty (12)$$

In the above equations, primes represent differentiation with respect to $\eta, \gamma = \frac{k_1 Le}{a}$is the chemical reaction parameter, $M = \frac{Re_a \sigma B_0^2}{Re_b^{\frac{1}{r+1}}}$ for magnetic parameter, $R = \frac{16\sigma T_\infty^3}{3k\rho C_p}$ for radiation parameter, $Le = \frac{\alpha}{D_B}$ Lewis number, $B = \frac{\tau D_B (C_f - C_\infty)}{\alpha}$is the Brownian motion parameter,$T_p = \frac{\tau D_T (T_f - T_\infty)}{T_\infty \alpha}$is the thermophoresis parameter, $P = \frac{XU}{\alpha} Re_b^{\frac{2}{r+1}}$ for the generalized Prandtl number, $A = \frac{Re_b^{\frac{2}{r+1}}}{Re_a}$ material parameter of the Sisko fluid, $Re_a = \frac{\rho x U}{a}$, and $Re_b = \frac{\rho x^r U^{2-r}}{b}$ are the local Reynolds numbers, a, b, and r are the material constants of the Sisko fluid, and $B_{i_1} = \frac{h_f}{k} x Re_b$ isthe generalized thermal Biot number. The physical quantities of interest are the Local skin friction, C_{fx}Nusselt number, N_{ux} and Sherwood number, Sh_x. These are expressed as.

$$C_{fx} = \frac{\tau_w}{\frac{1}{2}\rho U^2}, N_{ux} = \frac{x q_w}{k(T_w - T_\infty)}, Sh_x = \frac{x j_w}{k(C_w - C_\infty)} (13)$$

Here τ_w, q_w, and j_w are the shear stress along the stretching surface, heat flux, and the surface mass flux respectively whose expressions are stated below as

$$\tau_w = \left(a + b\left|\frac{\partial u}{\partial y}\right|^{r-1}\right)\frac{\partial u}{\partial y} \qquad \text{at } y = 0$$

$$q_w = -k\frac{\partial T}{\partial y} + (q_r)_w \text{ at } y = 0 \quad (14)$$

$$j_w = -D_B \frac{\partial C}{\partial Y} \text{at} \qquad \text{y s= 0s}$$

PluggingEqs. (6) and (7) in (13) we have the non-dimensional forms as

$$\frac{1}{2} Re_b^{\frac{1}{r+1}} C_{fx} = A f''(0) - [f''(0)]^r (15)$$

$$Re_b^{-\frac{1}{r+1}} N_{ux} = -\theta'(0) (16)$$

$$Re_b^{-\frac{1}{r+1}} Sh_x = -\varphi'(0) (17)$$

3.Method of solution

The Runge-Kutta-Fehlberg fourth-order methodcombined with the shooting method is used to solve the set of nonlinear boundary value problems inEqs. (9)– (11) subject to the boundary conditions (12) in view of [28]. Using transformational variables, Eqs. (9), (10), and (11)subject to Eq. (12) are transformed into a system of first-order ODEs in Eqs. (19), (21), and (23) with condition (24).

$$f = y_1, f' = y_2, f'' = y_3, f''' = yy_1 \quad (18)$$

$$yy_1 = \frac{-1}{A+r(y_3)^{r-1}}\left[\left(\frac{2(2r-)+1}{r+1}\right)y_1y_3 - sy_2^2 - My_2\right] \quad (19)$$

$$\theta = y_4, \theta' = y_5, \theta'' = yy_2 \quad (20)$$

$$yy_2 = \frac{-1}{1+R}\left[P\left(\frac{2(r-1)+1}{r+1}\right)y_1y_5 + By_7y_5 + T_py_5^2\right] \quad (21)$$

$$\varphi = y_6, \ \varphi' = y_{7,}\varphi'' = yy_3 \quad (22)$$

$$yy_3 = -L_e\left(\frac{2(r-1)+1}{r+1}\right)y_1y_7 - \frac{T_P}{B}yy_2 + \gamma y_6 \quad (23)$$

The associated boundary conditions are.

$$y_1(0), y_2(0) - 1, y_5(0) + B_{i_1}[1 - y_4(0)], y_2 \to 0, y_4 \to 0, y_6 \to 0 \ as \ \eta \to \infty \quad (24)$$

The set of discretizedEqs. (19), (21), and (23) with boundary condition, Eq. (24), is solved numerically using a shooting algorithm with a Runge-Kutta Feldberg integration scheme. This method involves transforming the problem into initial values that must be determined through guessing, and a fourth order Runge – Kutta iteration scheme is employed to integrate the set of initial value problems until the given boundary conditions are satisfied. The computational procedure was implemented using the Maple solver.

4.Results and Discussions

This section discusses the main properties of the physical parameters presented in Eqs. (9) through (11). These include the thermophoresis parameter, generalized Prandtl number, Lewis number, Brownian motion parameter, magnetic parameter, and temperature-dependent Biot number, among others.

Table 1 depicts a comparative analysis of the reduced Nusselt number compared to the results declared and published by [26, 5, 17, & 27]. The values have been compared with various values of P for 0.7, 0.2, 7.0, and 20.0, respectively. The table revealed that the present results agree well with the earlier published works as cited.

For different values of the magnetic field parameter, the velocity field is plotted against the similarity variable in Figs. 2 and 3. The figures show that, for both linear and nonlinear stretching

sheets, the velocity decreases as the magnetic field parameter (i.e., the ratio of electromagnetic force to viscous force) increases. The impact of the magnetic field parameter *M* on the fluid temperature and concentration is shown in Figs. 4, 5, 6, and 7. As depicted in the profiles, increasing magnetic field strength favors an increase in fluid temperature and concentration. This is because of the Lorentz force, which is a resistive force created when a magnetic field is introduced to an electrically conducting fluid. The velocity of the boundary layer fluid was reduced by this force. The magnetic field, *M*, is observed as thermal energy in addition to the additional work required to drag the conducting nanofluid against the action of the magnetic field. In the presence of a magnetic field, the thickness of the thermal boundary layer increases, whereas the thickness of the momentum boundary layer decreases.

For nonlinear stretching sheets with $r = 2$, Fig. 8 shows the effect of changing the generalized Prandtl number *P* on the dimensionless temperature. The temperature profile and related boundary thickness decreases as the Prandtl number increases. The thermal diffusivity weakens when the Prandtl number *P* continues to increase. Larger Prandtl numbers have poorer thermal diffusivity from a physical standpoint, while smaller Prandtl numbers have better thermal diffusivity. The temperature and thermal boundary layer are reduced owing to the gradient between the effects of high and low Prandtl numbers on thermal diffusivity. The effect of various *Le* values on the concentration profile of the nonlinear stretching sheet is shown in Fig. 9. Recall that, in the boundary layer phase,*Le* quantifies the ratio of the thermal diffusion rate to species diffusion rate. The figures demonstrate that when Le increases, the thermal boundary layer thickness decreases and were accompanied by a decrease in temperature and mass transfer. Further, this shows how increasing Le affects the concentration distribution significantly. As Le increases, the volume fraction boundary layer decreases across the plate. Figs. 10 and 11 show the effect of various values of the thermophoresis parameter T_p on the dimensionless temperature and concentration.

While Figs. 12 and 13 depict the influence of Brownian motion parameters for r = 2, Figs. 10 and 11 illustrate the effect of different values of the thermophoresis parameter Tp on the dimensionless temperature and concentration. As shown in the graphs, a drop in the Brownian motion parameter results in a decrease in the temperature profile and an increase in the concentration profile for the nonlinear stretching sheet. However, when the thermophoresis parameter is lowered, the concentration and temperature profiles both drops. The effect of lowering the Biot number on the Sisko nanofluid concentration is displayed in Figs. 13 and 14. As the Biots number declines, so does the fluid's concentration.

Additionally, Figs. 15 and 16 illustrate how various chemical reaction parameter values for species consumption and generation instances affect the dimensionless concentration for $r = 2$. In the given situations, it is observed that the concentration decreases for the constructive chemical reaction parameter and increases for the destructive chemical reaction parameter. This is because the molecule is consumed during systemic chemical processes, which lowers its concentration profile. The primary result is that the overshot in the profiles of solute concentration in the solute boundary layer can be reduced by a first-order chemical reaction.

The impact of varying the Sisko nanofluid material parameter value, A, on the dimensionless velocity profile is demonstrated in Figure 17. Recall that the material parameter A represents the high shear rate viscosity (consistency index). The graph clearly shows that the velocity distribution increases with the Sisko nanofluid material parameter, A. The reason being that when the material parameter A rises, the fluid's viscosity, or consistency index, decreases, thereby increasing the fluid's velocity. Figure 18 shows the effect of thermal radiation on the temperature profile (r = 2) for the nonlinear sheet. The profiles unequivocally demonstrate that the temperature dispersion widens as R decreases. This suggests that a decrease in the thermal radiation parameter favors an increase in the fluid's boundary layer thickness. Figures 19 and 20 illustrate the effects of the nonlinear stretching parameter (r) on the temperature and velocity distributions, respectively. It is obvious that while an increase in r barely affects the velocity profile, the temperature profile of the nanofluid also rises quickly. ed in Figure 17. Recall that the material parameter A represents the high shear rate viscosity (consistency index). The graph clearly shows that the velocity distribution increases with the Sisko nanofluid material parameter, A. The reason for this is that when the material parameter A rises, the fluid's viscosity, or consistency index, decreases, thereby increasing the fluid's velocity. Figure 18 shows the effect of thermal radiation on the temperature profile (r = 2) for the nonlinear sheet. The profiles unequivocally demonstrate that the temperature dispersion widens as R decreases. This suggests that a decrease in the thermal radiation parameter favors an increase in the fluid's boundary layer thickness. Figures 19 and 20 illustrate the effects of the nonlinear stretching parameter (r) on the temperature and velocity distributions, respectively. It is obvious that

while an increase in r barely affects the velocity profile, the temperature profile of the nanofluid also rises quickly.

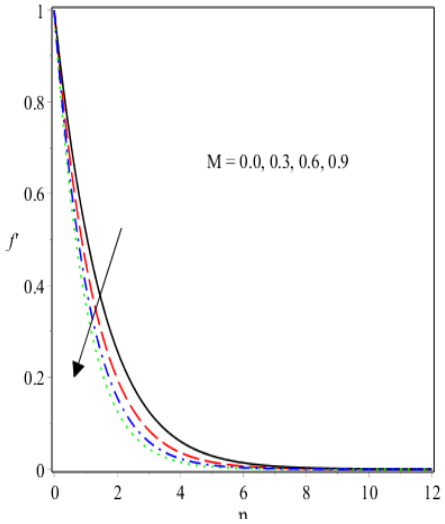

Fig. 2 Effect of Mon velocity($r = 1$)

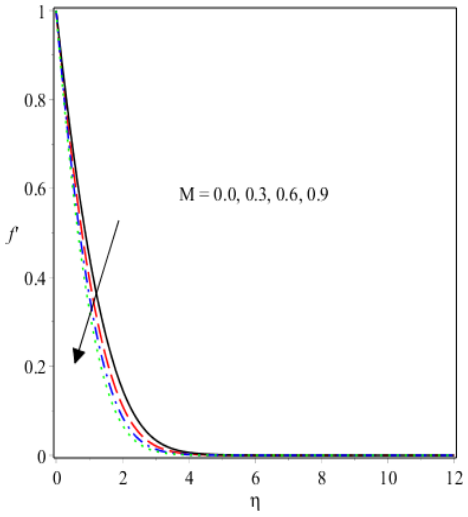

Fig. 3 Effect of M velocity profile($r = 2$)

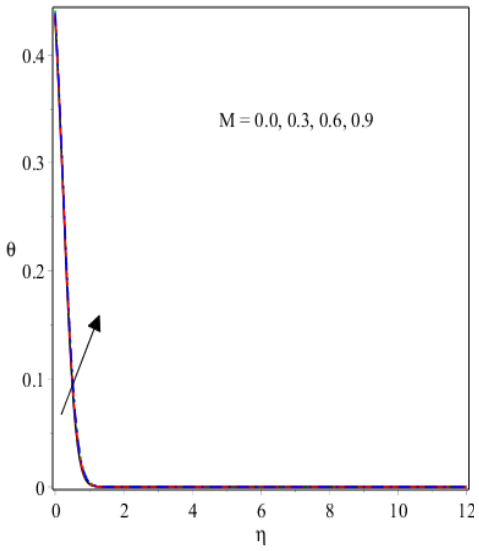

Fig. 4 Effects of M on temperature($r = 1$)

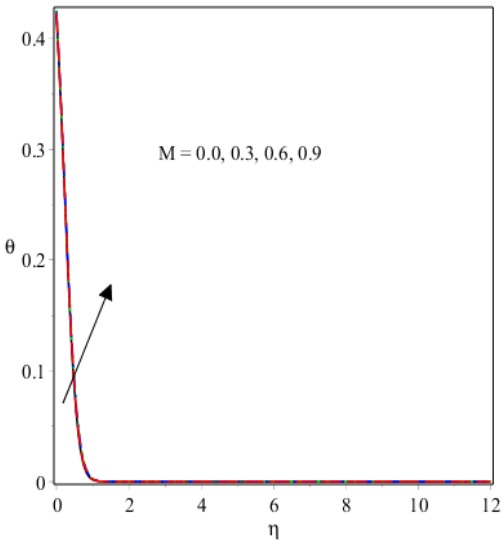

Fig. 5 Effects of M temperature($r = 2$)

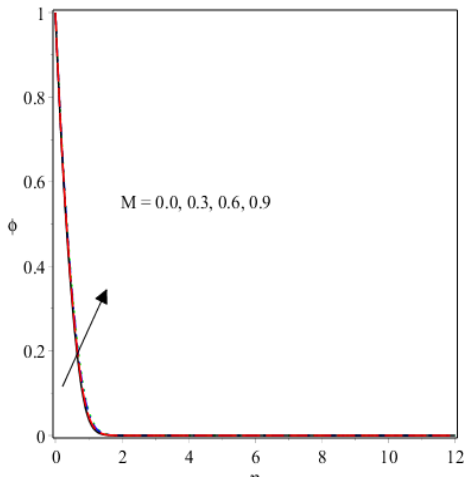

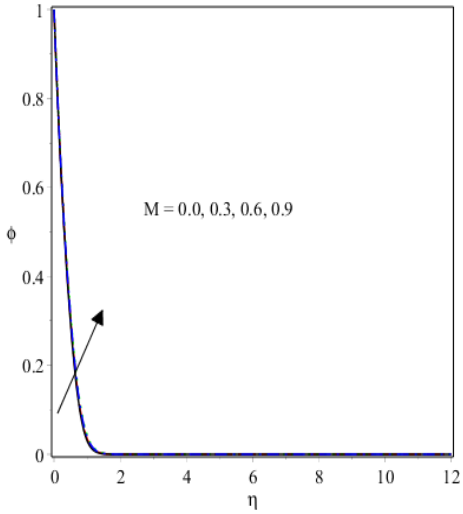

Fig. 6 Effects of M on concentration (r= 1)

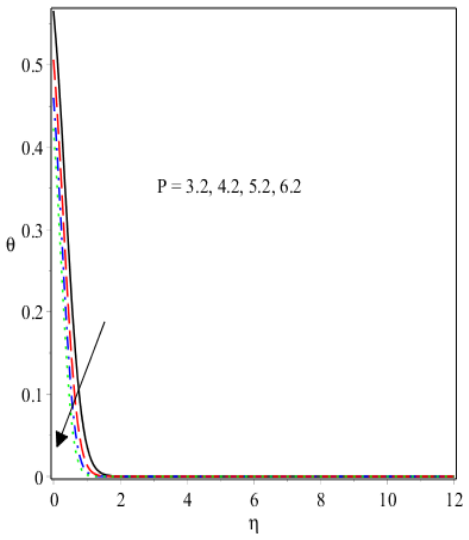

Fig. 7 Effects of *M*concentration ($r = 2$)

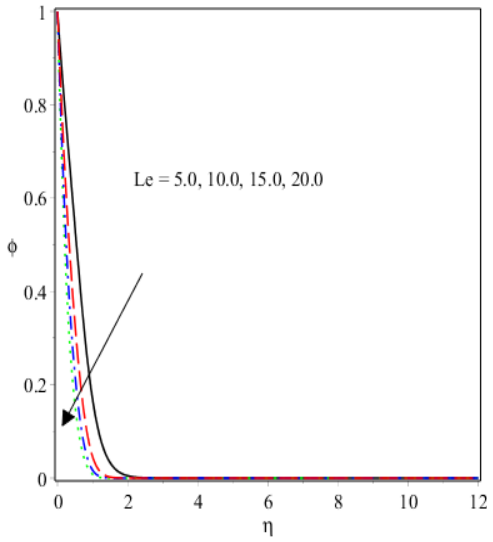

Fig. 8 Effect of *P* on temperature ($r = 2$)

Fig.9 Effect of varying *Le* concentration ($r = 2$)

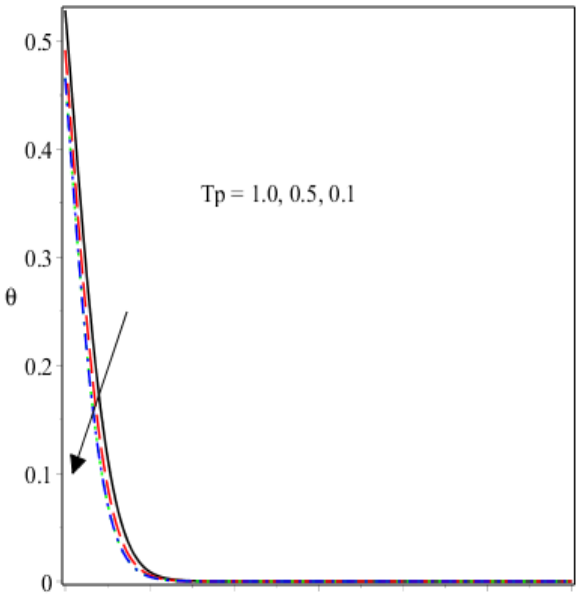

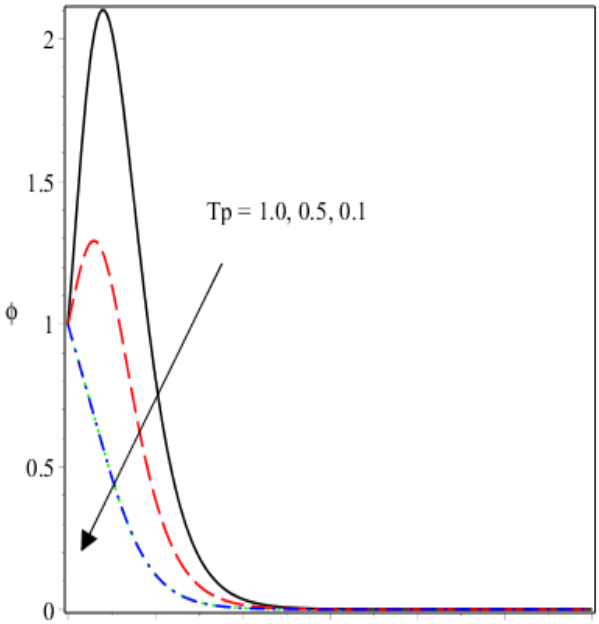

Fig. 10 Effect ofvarying temperature($r = 2$)

Fig. 11 Effect of varying T concentration ($r = 2$)

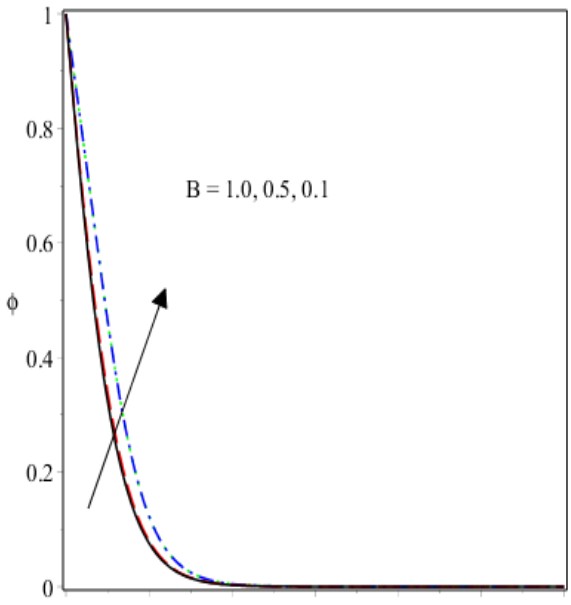

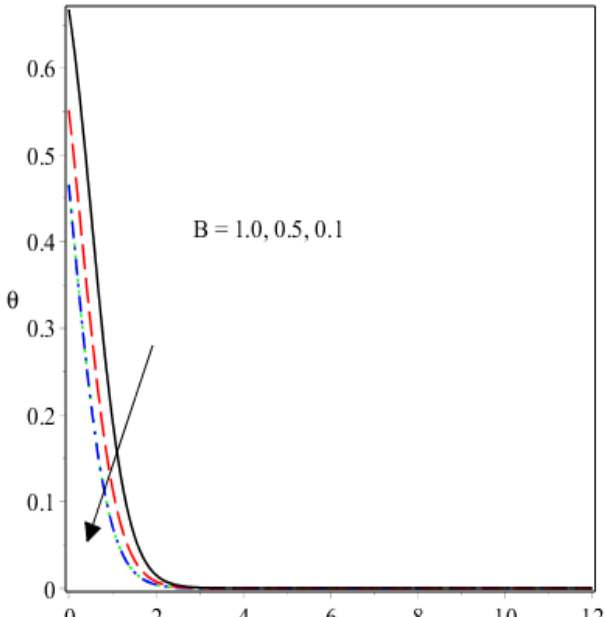

Fig. 12 Effect of B on concentration($r = 2$)

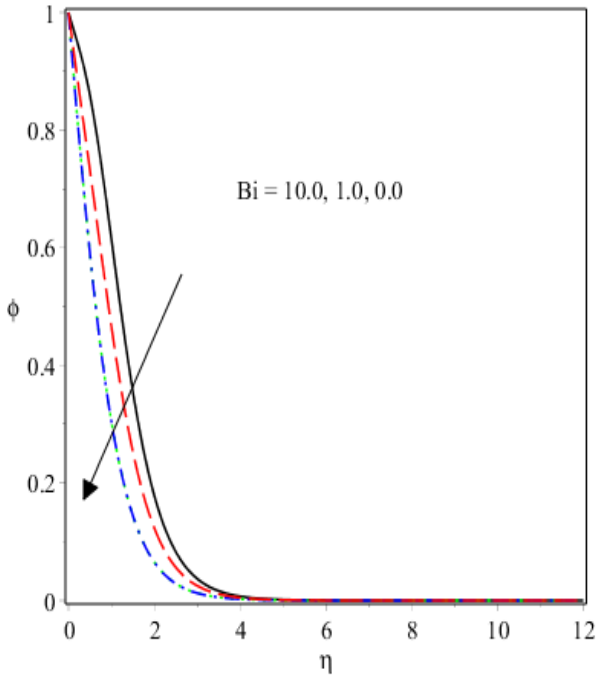

Fig 13 Effect of B temperature ($r = 2$)

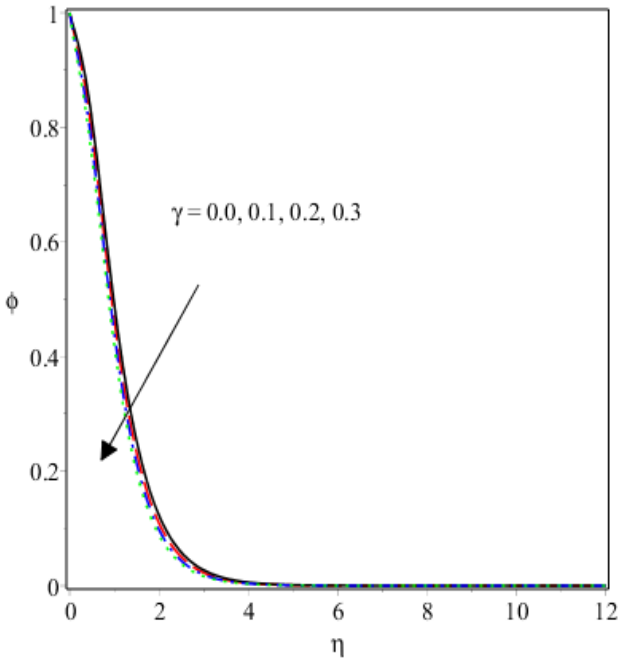

Fig. 14 Effect of Bion concentration($r = 2$)

Fig.15.Effect of γ on concentration ($r = 2, Le = 2.0$)

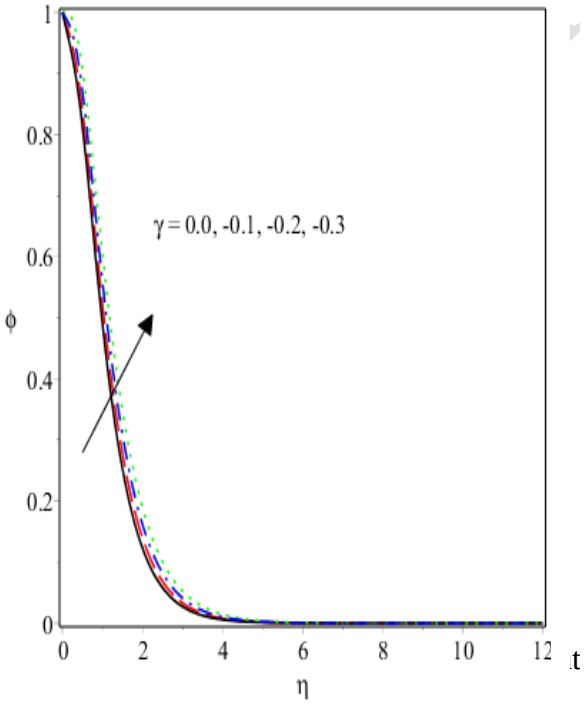

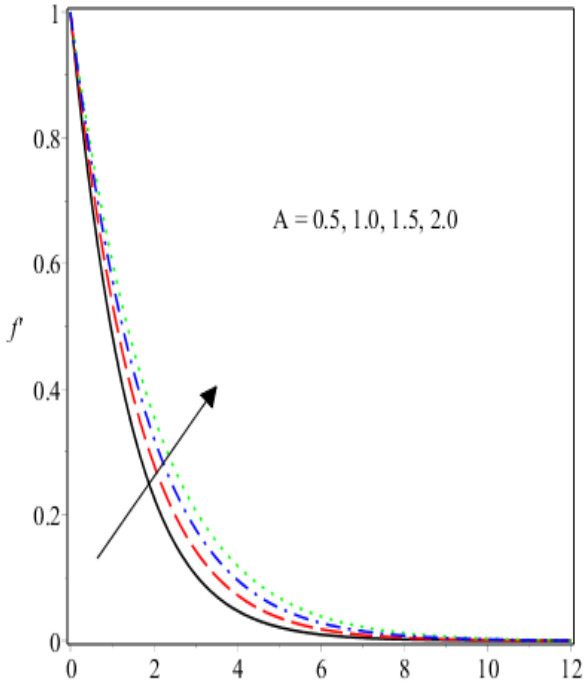

Fig. 16 Effect of γ on concentration ($r = 2, Le = 2$)

Fig. 17 Impact of Aon velocity profile

Fig. 18 Influence of *R* temperature $(r = 2)$ Fig. 19 Influence of *r* on temperature

Sssss

Fig. 18 Influence of *R* temperature $(r = 2)$ Fig. 19 Influence of *r* on temperature

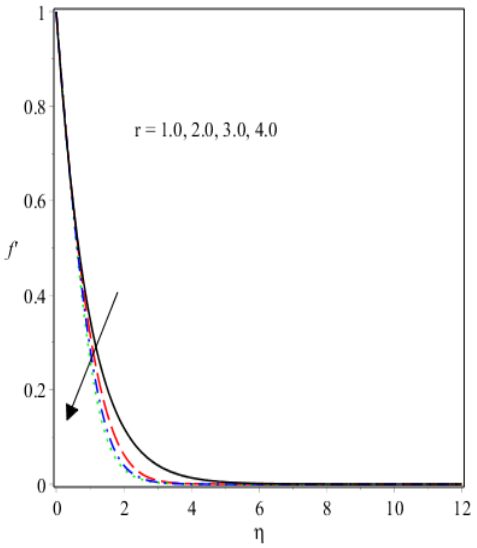

Fig 20.Influence of*r* on Velocity profile

Table 1 Comparison of results for reduced Nusselt number $-\theta'(0)$ for $A = B = M = R = B_{i1} = S = 0$

P	Masood [26]	Khan& Shahzad [5]	Prasanna kumara et.al [17]	Venkatta et.al [27]	Present results
0.7	0.4539	0.4539	0.4544	0.454470	0.36234
2.0	0.9113	0.9113	0.9113	0.911353	0.78345
7.0	1.8954	1.8954	1.8954	1.895400	1.75342
20.0	3.35395	3.3539	3.3539	3.353902	3.37234

5.Concluding Remarks

The effect MHD on the flowof a Sisko nanofluid with mass transfer under a nonlinear stretching sheet was investigated. The effects of the pertinent parameters on the dimensionless velocity, dimensionless temperature, and dimensionless concentration are considered and presented graphically. The following conclusions are drawn from our study.

- As the material parameter and magnetic field of the Sisko nanofluid increases, the velocity profile experiences a sharp decline.
- Increasing *M* and *r* enhances the temperature profile.
- There is enhancement of concentration as a result of increased magnetic field parameters. This is also observed in the case of the destructive chemical reaction parameter, where the concentration is enhanced.
- Increase in *P* lead to a decrease in the temperature profile.
- The temperature and concentration profiles decrease as the Brownian motion decreases.
- A decrease in the Biot number decreases the fluid's concentration while increasing the temperature profile.
- Decreasing the thermophoresis parameter favors a decrease in both concentration and temperature profiles.
- Increasing Lewis number significantly decreased the volume fraction of the boundary layer across the plate.

References

1. Sisko, J.(2010). Shear Thinning Nanofluids. US Patent No. 7,772,012.

2. Sisko, J. Zhang, D. (2012).Experimental investigation of the rheological behavior of shear-thinning nanofluids. Journal of Nanoparticle Research, 14(1), 1-10.

3. Sisko, J, Zhang, D. (2014). Heat transfer and flow characteristics of shear-thinning nanofluids. International Journal of Heat and Mass Transfer, 77, 115-123.

4. Sisko, J,Zhang, D. (2016). A review on the rheological behavior of shear-thinning nanofluids. Journal of Nanofluids, 5(1), 1-17.

5. Khan M, Shahzad, A. (2013). On boundary layer flow of Sisko fluid over stretching sheet. QuaestionesMathematicae, Volume3, (5), 137–51.

6. Malik R, Khan M, Munir A, Khan W,A. (2014). Flow and heat transfer in Sisko fluid withconvective boundary condition. PLOS ONE,9(10), 107989.

7. Nandeppanavar M, M., Vajravelu K, Subhas Abel, M. Chiu-On N (2011). Heat transfer over anonlinearly stretching sheet with non-uniform heat source and variable walltemperature.Int J Heat Mass Transfer, 54, (5), pp. 23–36.

8. Ahmad A, Asghar, S.(2012). Flowand heat transfer over hyperbolic stretching sheets. AppliedMathematicsand computation33(4):445–54.

9. Murshed F, K., Chowdhury I, R (2015). Chattopadhyay A, Sandeep N. Radiation effect on boundary layer flow of a nanofluid over a nonlinearly permeable stretching sheet.Adv Phys Theor Appl, 40, 2225–0638.

10. Rashidi M, M., Momoniat E, Ferdows M, Basiriparsa A. (2014). Lie group solution for freeconvective flow of a nanofluid past a chemically reacting horizontal plate in aporous media. Article ID 239082 Math Problems Eng.

11. Mondal H, Mishra S, Bera U, K. (2015). Nanofluids on MHD mixed convective heat and mass transfer over a nonlinear stretching surface with suction/injection.J Nanofluids,4(2):223–9.

12. Dhanai R, Rana P, Kumar, L. (2015). Multiple solutions of MHD boundary layer flow and heat transfer behavior of nanofluids induced by a power-law stretching/shrinking. Permeable sheet with viscous dissipation. Powder Technol, 273, 62–70.

13. Das, K. (2015). Nanofluid flow over a nonlinear permeable stretching sheet with Partial slip.Journal of Egyptian Mathematical Society, 23, 451–466.

14. Megahed A, M. (2015). Flow and heat transfer of a non-Newtonian power-law fluidover a nonlinearly stretching vertical surface with heat flux and thermal radiation, Mechanica, 50(7), 1693–700.

15. Gnaneswara R, M., Padma P, Shankar B, Gireesha B, J. (2016). Thermal radiation effects onMHDstagnation point flow of nanofluid over a stretching sheet in a porous medium.J Nanofluids, 5(5), 753–64.

16. Magyari E, Pantokratoras A. (2011). Note on the effect of thermal radiation in the linearizedRosseland approximation on the heat transfer characteristics of various boundary layer flows. Int Commun Heat Mass Transfer, 38, 554–656.

17. Prasannakumara, B, C.,Gireesha, B, J., Krishnamurthy, M, R. (2017). Ganesh Kumar, K. MHD flow and nonlinear radiative heat transfer of Sisko nanofluid over a nonlinear stretching sheet. Informatics in Medicine Unlocked, 9, 123-132.

18. Nagendramma, V. (2020). Magnetohydrodynamic chemically reactive Sisko liquid flow through a stretching surface with nonlinear thermal radiation., Journal of Physics Conference Series, 15597, 012037.

19. Parida S, K., Panda S, Rout, B,R.(2015). MHD boundary layer slip flow and radiative nonlinearheattransfer over a flat plate with variable fluid properties and thermophoresis.Alexandria Eng J, 54(4), 941–953.

20. Cortell,R.(2014). Fluid flow and radiative nonlinear heat transfer over a stretching sheet. J King Saud Univ – Sci, 26, 161–177.

21. Pantokratoras, A. (2014). Natural convection along a vertical isothermal plate with linear and nonlinear Rosseland thermal radiation. Int J Therm Sci, 84, 151–165.

22. Hayat T, Muhammad T, Shehzad S, A., Alsaedi A. (2015). Three-dimensional flow of Jeffrey nanofluid with a new mass flux condition.Aerospace Engineering,1061/(ASCE)AS.1943-5525.0000549J, 04015054.

23. Khan M, Malik R, Munir A, Khan W, A. (2015). Flow and heat transfer to Sisko nanofluid overa nonlinear stretching sheet. PLOS ONE 2015;10(5):0125683. http://dx.doi.org/10.1371/journal.pone.0125683.

24. Mabood F, Ibrahim S, M, Rashidi M, M.,Shadloo M, S., Lorenzini, G. (2016). Non-uniform heat source/sink and Soret effects on MHD non-Darcian convective flow past a stretching sheet in a micropolar fluid with radiation.Int J Heat Mass Transfer, 93, 674–82.

25. Ebiwareme, L, Bunonyo, K, W., Davies, O, A. (2023). Analytical solution for heat and mass transfer of two-phase nanofluid flow with magnetic field in a rotating system using Adomian decomposition method.International Journal of Scientific and innovative mathematical research, Volume 11, Issue 2, pp. 1-16.

26. Masood, K, Rabia, M., Munir, Waqar Azeem, K. (2015). Flow and Heat transfer of Sisko nanofluid over a nonlinear stretching sheet.PLOS ONE.

27. Venkatta R, G., Sreedhar B, M.,Lavanaya, M. (2016). Convective heat and mass transfer flow of Sisko nanofluid past a nonlinear stretching with thermal radiation. International Refereed Journal of Engineering and Science, Volume 5, Issue 2, pp. 17-37.

28. Malik, R,Khan, M, Munir, A, Khan W, A. (2014). Flow and Heat Transfer of Sisko Fluidwith convective Boundary Condition (2014). PLOS ONE 9(10): e107989, Doi: 10.1371/journal.pone.0107989 PMID: 25285822

29. Munir, A, Shahzad, A, Khan, M. (2014). Forced Convective heat transfer in boundary layer flow of Sisko fluid over a nonlinear stretching sheet. (2014) PLOS ONE 9(6): Doi: 10.1371/journal.pone.0100056 PMID: 24949738,e100056.

30. Pal, D., Mandal, G. (2020). Magnetohydrodynamic stagnation-point flow of Sisko nanofluid over a stretching sheet with suction. Propulsion and Power Research, Volume 9, Issue 4, Pages 408-422.

31. Mahmood, T., Igbal, Z., Ahmed, J., Shahzad, A., Khan, AM. (2017). Combined effects of magnetohydrodynamics and radiation on a nano Sisko nanofluid fluid towards a nonlinear stretching sheet. Results in Physics, Elsevier. Volume 7, Pages 2458-2469.

32. Nareender, G., Govardhan, K., Sreedhar, Sarma, G. (2020). Numerical study of radiative magnetohydrodynamics viscous nanofluid due to convective stretching sheet with chemical reaction, PLOS One, Volume 16, Issue 6, Pages 2165-2179.

33. Macha, M., Gireesha, B. J., Kishan, N. (2019). Magnetohydrodynamics boundary layer flow and heat transfer of Sisko nanofluid past a nonlinearly stretching sheet with thermal radiation. Applications and Applied Mathematics, Volume 14, Issue 4, PP. 1-15.

34. Ankita, B., Arvind Singh, B. (2022). Radiative heat transfers due to Solar radiation on magnetohydrodynamics Sisko nanofluid. Japanese Research, Volume 51, Issue 8, pp. 7411-7434.

35. Hayat, T., Hussain, M., Alsaedi, A., Shehzad, S. A., Chen, G. O. (2017). Flow of Power-law nanofluid over a stretching surface with Newtonian heating. Journal of Applied Fluid mechanics, Volume 8, No. 2, pp. 273-280.

Nomenclature

u, v	Velocity components along x and y
D_B	Brownian diffusion coefficients
D_T	Thermophoresis diffusion coefficient
f'	Nondimensional velocity
Re_a, Re_b	Local Reynold numbers
Nu_x	Local Nusselt number
Sh_x	Local Sherwood number
Le	Lewis number
Pr	Prandtl number
B	Brownian motion
T_p	Thermophoresis parameter
A	Sisko fluid parameter
Bi_1	Thermal Biot numbers
Cf_x	Local Skin friction
M	Magnetic field
R	Radiation parameter
B_0	Induced magnetic field.

T_∞	Ambient temperature
C_w	Concentration of the walls
C_∞	Ambient concentration
C_p	Specific heat capacity of nanoparticles at constant pressure.
a, b	Material constants of the fluid
r	Power law index
U	Stretching sheet velocity
T_w	Uniform wall temperature
k_1	Chemical reaction coefficient
q_w	Heat transfer
j_w	Surface mass flux
s	Stretching rate
T	Temperature of the fluid
C	Concentration of the fluid
x, y	Direction of velocity along and perpendicular to the plate

Greek Letters

α	Fluid thermal diffusivity
θ	Dimensionless temperature of the fluid
φ	Dimensionless Concentration
γ	Chemical reaction parameter
η	Similarity variable
ρ_f	Fluid density
σ	Electrical conductivity of the fluids
κ	Thermal conductivity
υ	Kinematic viscosity
ψ	Stream function
τ	Ratio of the effective heat capacity of the nanoparticles to heat capacity of the fluid.